

Fatigue strength of submicrocrystalline Ti and Zr-2.5%Nb alloy after equal channel angular pressing

V. F. Terentyev¹, S. V. Dobatkin^{1,2*}, S. A. Nikulin², V. I. Kopylov³, D. V. Prosvirnin¹,
S. O. Rogachev², I. O. Bannykh¹

¹*A. A. Baikov Institute of Metallurgy and Materials Science of RAS, Leninskiy prospect 49, 119991 Moscow, Russia*

²*National University of Science and Technology MISIS, Leninskiy prospect 4, 119049 Moscow, Russia*

³*Physico-Technical Institute of NAS Belarus, ul. Kuprevicha 10, 220141 Minsk, Belarus*

Received 1 July 2010, received in revised form 12 October 2010, accepted 12 October 2010

Abstract

The static and fatigue strength properties of commercially pure VT1-00 (Russian standard) titanium and the Zr-2.5%Nb zirconium alloy have been studied after equal-channel angular pressing (ECAP). It is shown that the formation of submicrocrystalline (SMC) structure upon ECAP leads to significant strengthening, increases the service life in a high stress amplitude range and increases the fatigue strength relative to those typical of the annealed state. The specific features of the fatigue fracture mechanism in different structural states of materials are studied.

Key words: titanium, Zr-2.5%Nb zirconium alloy, severe plastic deformation, submicrocrystalline structure, fatigue strength, propagation of fatigue cracks

1. Introduction

At present, the titanium alloys characterized by high biocompatibility with human body tissues and high mechanical properties are predominantly used for medical tools, for dental and orthopaedic implants and endoprosthetics, and in neurosurgery and oncology. The application of zirconium alloys in medicine is limited because their strength properties are lower than those of titanium alloys despite the fact that the biocompatibility of zirconium alloys with the human body is better [1–4]. Strengthening of zirconium alloys significantly widens their application for medical equipment since their inert behaviour in the body tissues does not affect the human health. The conventional methods of the strengthening of zirconium alloys do not provide the strength level of titanium alloys [5, 6]. In the present work, the strengthening of zirconium alloys is achieved due to the ultrafine-grained (nanostructured or submicrocrystalline) state obtained in them by the methods of severe plastic deformation (SPD). There are few data on the structure and properties of zirconium and its alloys after SPD

in literature, and such data are generally obtained on small samples upon high pressure torsion [7, 8]. Only structure examination was performed in the case of equal-channel angular pressing (ECAP) [9, 10]. However, numerous studies of other metals and alloys in nanostructured and submicrocrystalline states show a substantial increase (by a factor of 2–8) in the strength properties relative to those observed in the initial state [11].

In addition to the high strength and biocompatibility, high fatigue strength is necessary for the application of metal for medical equipment. For increasing the strength properties of titanium and its alloys upon static deformation and fatigue load, these characteristics have been studied under the effect of SPD, in particular, ECAP, and additional thermomechanical treatments [12–19]. As a rule, SPD improves the static and fatigue mechanical properties, but it was observed that the correlation between improvements in the static and cyclic characteristics of fracture after SPD is not always unambiguous.

The purpose of this work was the comparative study of the effect of ECAP on the static and cyc-

*Corresponding author: tel.: +7 499 1357743; fax: +7 499 1358680; e-mail address: dobatkin@imet.ac.ru

lic strength characteristics of titanium and the Zr-2.5%Nb zirconium alloy.

The Zr-2.5%Nb zirconium alloy selected for the study is widely used for the critical elements of the active zone of atomic power reactors [5]. The Zr-2.5%Nb alloy is most acceptable among the existing industrial zirconium alloys for the preparation of medical implants. Compared with the Zr-2.5%Nb alloy, the multicomponent alloys containing iron, tin, and oxygen are characterized by worse biological sluggishness, and the binary Zr-1%Nb alloy has a lower strength [3].

2. Experimental procedure

Commercially pure VT1-00 (Russian standard) titanium and the Zr-2.5%Nb zirconium alloy were used for the study. The impurity contents in the VT1-00 titanium according to ASTM B265 were (wt.%) < 0.20 Fe; < 0.08 Si; < 0.10 O₂; < 0.04 N₂; < 0.008 H₂. The billets of $14 \times 14 \times 120$ mm³ in size for ECAP were preliminarily annealed at a temperature of 560 °C (for 2 h, cooling in furnace) for release of work hardening and internal stresses.

Bars of 20 mm in diameter from the Zr-2.5%Nb alloy (alloy E125 in Russian standard) containing (wt.%) 97.25 Zr, 2.7 Nb, 0.05 Fe were used after cold rolling and annealing at 530 °C (1 h). After annealing, the structure of the alloy is partially polygonized (with a subgrain size of 100–300 nm) and partially recrystallized (with a grain size of 1–5 μm). Pieces 120 mm long were cut from the bars of the alloy in the as-received condition and milled by hard-alloy head to a size of 14×14 mm², which corresponds to the size of the working channel of the tool for isothermal ECA pressing.

ECA pressing of VT1-00 titanium and Zr-2.5%Nb alloy was performed under isothermal conditions at a temperature of 420 °C with an angle of 90° between channels by the route close to B_c by 4 (for the Zr-2.5%Nb alloy) and 6 (for the VT1-00 titanium) passes corresponding to a true (logarithmic) strain of 2.1 and 2.5, respectively [20].

The static mechanical properties were determined with a 10-ton 3380 Instron mechanical testing machine. The fatigue tests under the conditions of repeated tension at a constant minimum stress of 30 MPa were performed with an E3000 Instron Electro Puls pulser at a frequency of 30–40 Hz. Flat samples with a gage part of $1 \times 3.5 \times 16$ mm³ in size were spark cut from the billets. These samples were used for static and fatigue tests. The gage part surfaces of the samples were subjected to mechanical and chemical polishing, which ensured the mean arithmetic deviation of the profile irregularities (roughness) $R_a = 0.29$ μm.

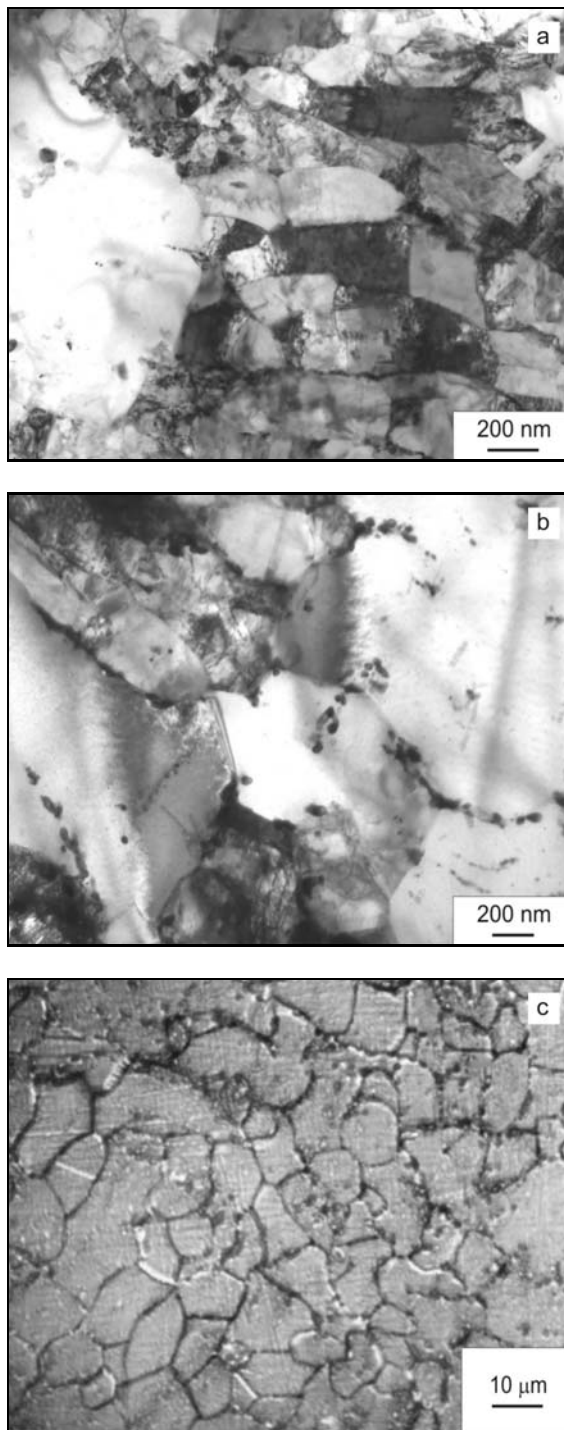


Fig. 1. Initial structure of the Zr-2.5%Nb alloy (a, b) and VT1-00 titanium (c).

3. Results and discussion

Structural state. Before ECAP, the Zr-2.5%Nb alloy after cold rolling and annealing at 530 °C (1 h) has a mixed structure, which is partially polygonized (with a subgrain size of 100–300 nm), and partially recrystallized (with a grain size of 1–5 μm) (Figs. 1a,b). The

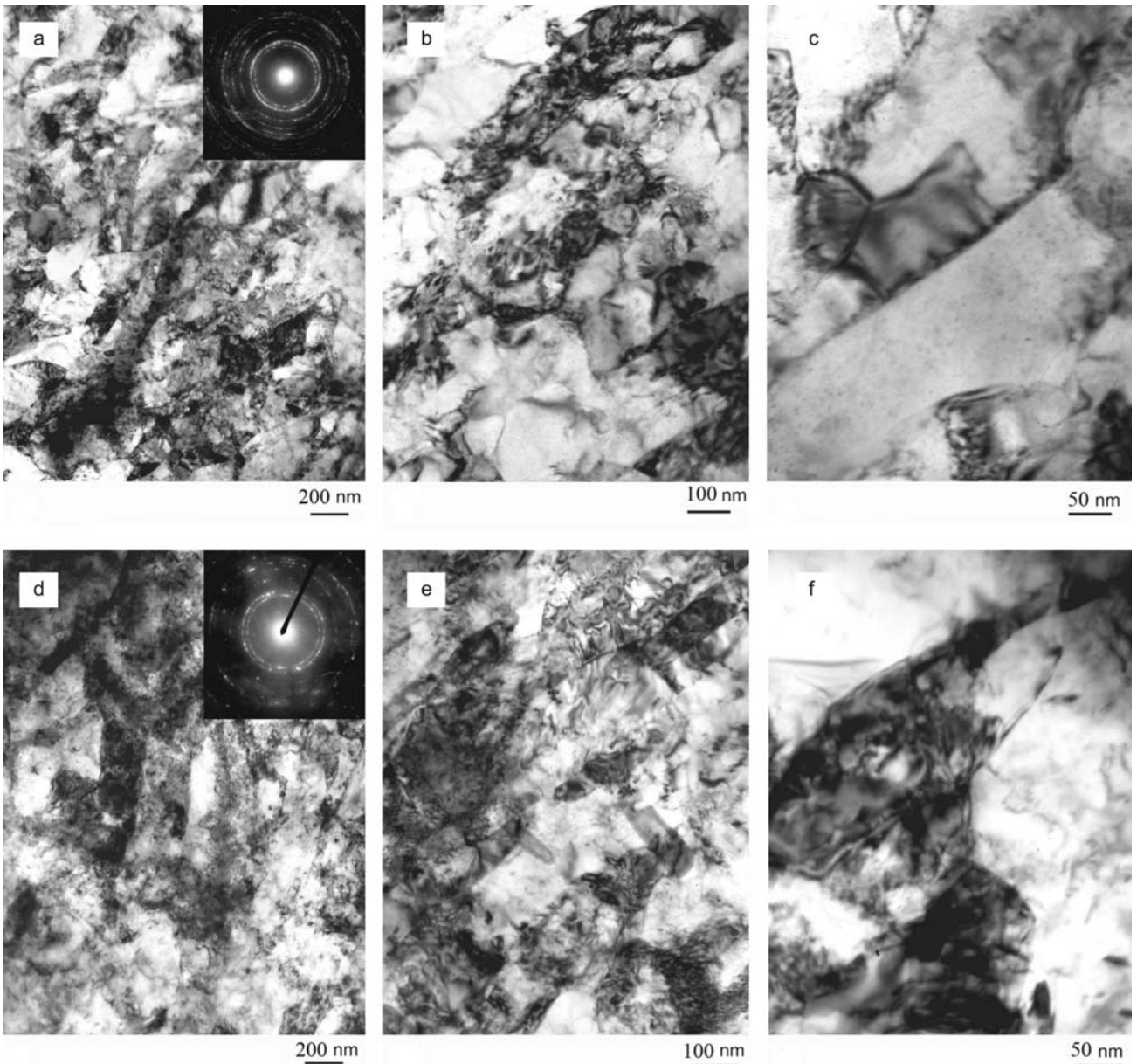


Fig. 2. Structure of the Zr-2.5%Nb alloy (a, b, c) and the VT1-00 titanium (d, e, f) after ECAP.

structure of the Zr-2.5%Nb alloy contains the β -Nb particles of 0.015–0.05 μm in size are arranged predominantly inside the α -Zr grains. The microstructure of the VT1-00 titanium in the initial state consists of equiaxed grains of 15 μm in average size (Fig. 1c).

The predominantly submicrocrystalline grained-subgrained structure of the Zr-2.5%Nb alloy after ECAP is similar to that of the VT1-00 titanium (Fig. 2). The structure is somewhat oriented as a consequence of the formation of elongated subgrains at the stage of unsteady polygonization [21] and/or shear bands at the early stages of ECAP. Upon low-temperature ECAP, the ultrafine-grained (UFG) structure is formed by the recrystallization mechanism similar to the Cahn-Burgers mechanism [22], i.e.,

through the coalescence of subgrains with some structure features characteristic of cold deformation, upon which, in addition to the cellular structure and subgrains, the oriented structure elements such as twins, deformation bands, shear bands, kink bands, etc. appear in the deformed grains [23], and the diffusion processes occur due to high pressure and high degree of deformation rather than at the expense of thermal activation [24]. The process of the subgrain growth due to their coalescence at the prerecrystallization stage is also called *continuous recrystallization* [25], *recrystallization “in situ”* [26], or *dynamic coalescent polygonization* [21, 27]. In our case, the transformation of the oriented subgrained structure into equiaxed grained structure occurs by the intersection of two systems

Table 1. Mechanical properties of titanium VT1-00 and zirconium alloy Zr-2.5%Nb after ECAP

Materials	States	YS (MPa)	UTS (MPa)	EL (%)	σ_R (MPa)	σ_R/UTS
Titanium VT1-00	Initial state	310	450	30.5	280	0.62
	After ECAP	641	739	11.4	400	0.54
Zr-2.5%Nb	Initial state	377	569	26.1	340	0.60
	After ECAP	622	771	9.7	420	0.54

Note: σ_R – the fatigue limit based on 10^7 cycles

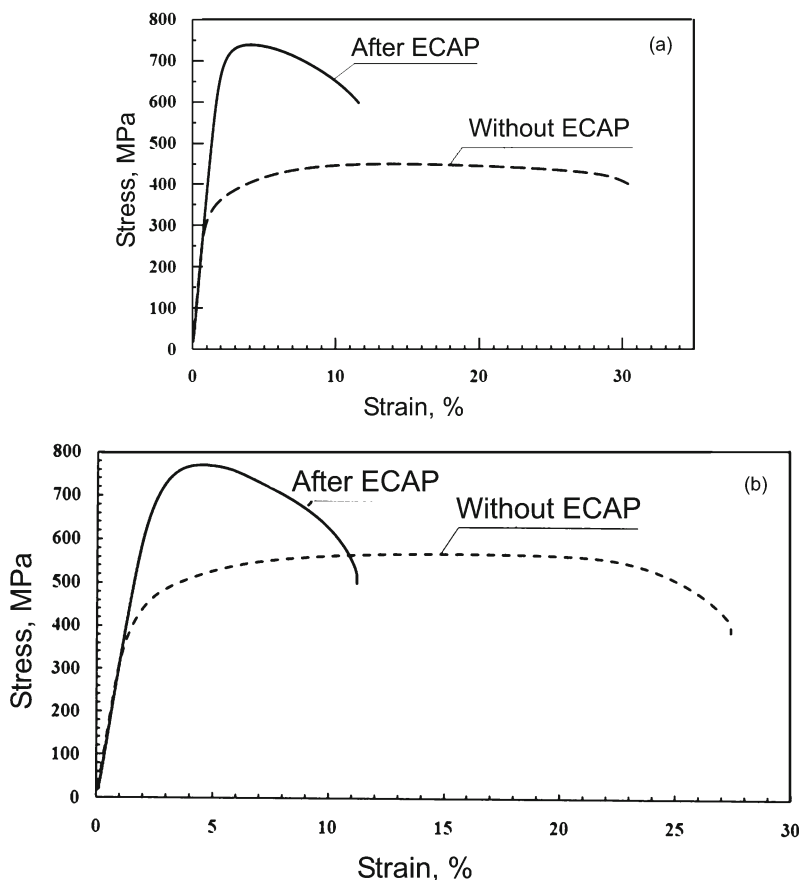


Fig. 3. Static tension curves of the VT1-00 titanium (a) and the Zr-2.5%Nb alloy (b) in different structural states.

of structure elements (subgrains, deformation bands) or by the formation of dislocation bridges in the oriented structure elements and the subsequent coalescence and “rounding” of subgrains (Fig. 2). According to quantitative structure estimation, the coalescence in the oriented subgrains can be multiple (Figs. 2b and 2e). The transverse size of the oriented structure elements in the Zr-2.5%Nb alloy and VT1-00 titanium after ECAP was 30–150 nm and 20–80 nm, respectively, and the size of the equiaxed grains (subgrains) was 50–200 nm and 50–170 nm, respectively. It is evident that the quantitative structure parameters in both materials are approximately identical. The presence of high-angle boundaries, i.e., the grained structure, was judged from the presence of the rings of point re-

flections in the electron diffraction patterns (Figs. 2a and 2d) and the banded contrast at the boundaries (Figs. 2b,c and 2e,f). The submicrocrystalline structure of the VT1-00 alloy after ECAP is less uniform and somewhat more oriented than that of the Zr-2.5%Nb alloy despite the fact that the degree of deformation upon ECAP of the VT1-00 titanium was higher than that of the Zr-2.5%Nb alloy.

Mechanical properties upon static tensile tests and fatigue tests. The static tension curves of the VT1-00 titanium and the Zr-2.5%Nb alloy are represented in Fig. 3, and the mechanical properties are given in Table 1.

It is evident from Table 1 that the yield strength and ultimate tensile strength of both materials after

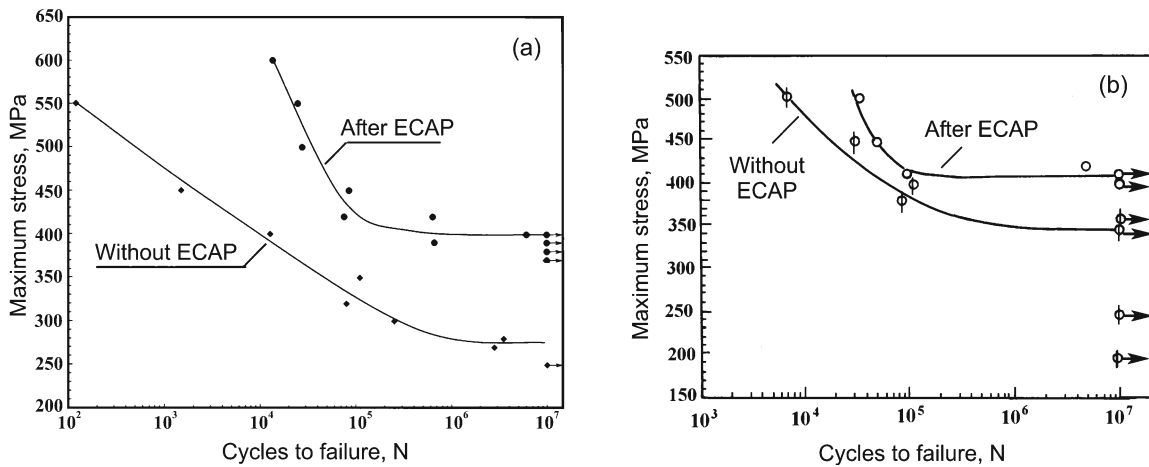


Fig. 4. Fatigue curves of commercially pure titanium VT1-00 (a) and the Zr-2.5%Nb alloy (b) in different structural states.

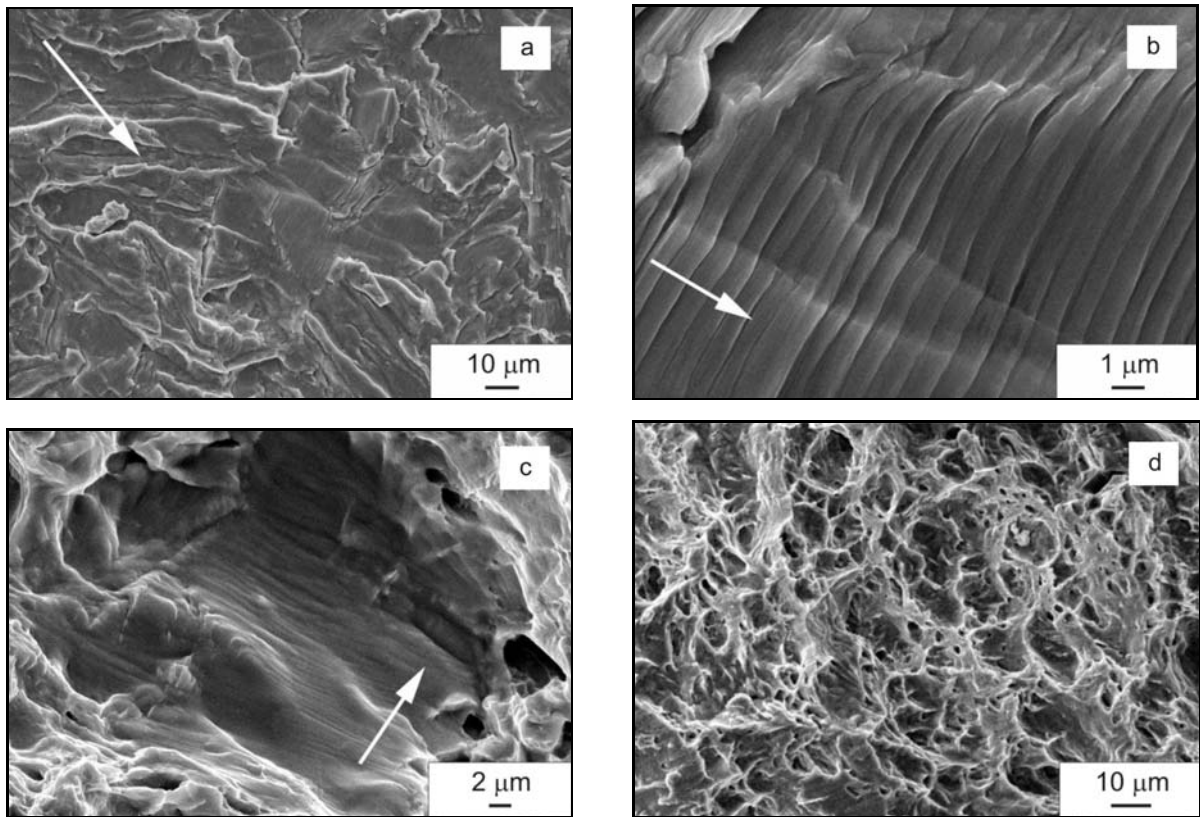


Fig. 5a–d. Fatigue fracture surfaces of the commercially pure VT1-00 titanium sample in the initial state: $\sigma_{\max} = 280$ MPa, $N = 3.5 \times 10^6$ cycles.

ECAP substantially increases, but the ductility decreases more than by a factor of two. Strain hardening of the VT1-00 titanium is higher than that of the Zr-2.5%Nb alloy, for example, the yield strength after ECAP increases by a factor of 2.1 in titanium and only by a factor of 1.6 in the zirconium alloy. This is explained by a high strength of the Zr-2.5%Nb alloy in the initial state due to a small initial grain size ($\sim 5 \mu\text{m}$) attained upon annealing at 530°C (1 h) be-

fore deformation. The ultimate tensile strength after ECAP is somewhat higher in the Zr-2.5%Nb alloy (Table 1).

The fatigue curves of the materials are represented in Fig. 4. As in the early works [18, 19, 28–32] devoted to the effect of ECAP on the fatigue characteristics of titanium, the fatigue strength of the VT1-00 titanium after ECAP in our work increases and reaches 400 MPa, i.e., becomes higher by ~ 120 MPa

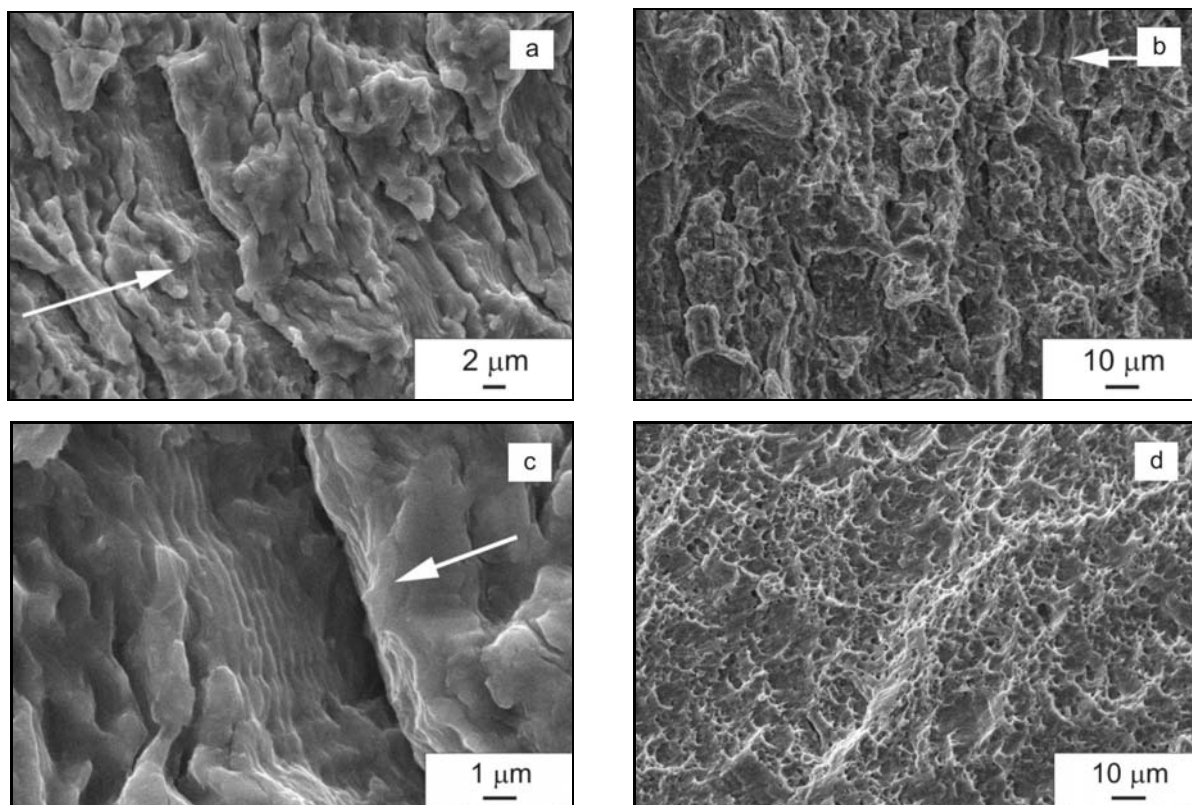


Fig. 6a–d. Fatigue fracture surfaces of the commercial VT1-00 titanium sample after ECAP: $\sigma_{\max} = 400$ MPa, $N = 6.1 \times 10^6$ cycles.

(or by a factor of 1.4) relative to that of the initial state, and the limited fatigue life at comparable stress levels increases more than by an order of magnitude (Fig. 4a). The endurance ratio σ_R/UTS (σ_R – fatigue limit) becomes 0.54, while in the initial state this ratio is 0.62.

The fatigue limit σ_R of the Zr-2.5%Nb alloy samples after ECAP is 420 MPa (Fig. 4b), i.e., it increases by 80 MPa (or by a factor of 1.2) in comparison with that of the initial state. The limited fatigue life of the Zr-2.5%Nb alloy samples after ECAP increases in several times in comparison with that of the samples in the initial structural state (Fig. 4b). Thus, the increase in the fatigue strength after ECAP in the Zr-2.5%Nb alloy is somewhat smaller than that of the VT1-00 titanium. This can be caused by the high fatigue strength of the fine-grained zirconium alloy in the initial state, but the σ_R value itself after ECAP is somewhat higher. The endurance ratio σ_R/UTS of the zirconium alloy is 0.54 after ECAP and 0.60 for the initial state; these values virtually coincide with those of the VT1-00 titanium.

Thus, it is apparent that ECAP of both materials leads to the achievement of close mechanical properties. As possible materials for bio-implants, they virtually do not have any advantages over each other in the level of mechanical characteristics. However, the

zirconium alloy provides better biocompatibility and, therefore, along with titanium, is a promising material for the medical industry.

Fractographic studies. The fractographic studies showed that the zone of the stable fatigue crack growth in the VT1-00 titanium in the initial state exhibits a sufficiently flat macrorelief of the fracture surface, on which grain boundaries are revealed (Fig. 5a). The crack propagation occurs with the formation of typical fatigue grooves; the distance between the grooves is $\sim 0.8 \mu\text{m}$ (Figs. 5a,b). In Fig. 5a, the general macroscopic direction of the fatigue crack propagation is shown by the arrow; however, this direction somewhat changes at the microlevel, depending on the orientation of individual grains. The accelerated growth of the fatigue crack exhibits a mixed pattern, in which the regions of ductile dimple fraction alternate with the regions of grooved relief with a spacing of 1–2 μm between the grooves (Fig. 5c). A typical ductile dimple fracture with a dimple size of 5–20 μm is observed in the static rupture area (Fig. 5d).

At the stage of the stable crack growth, a quasi-ductile irregular macro-grooved relief, which resembles lamellar relief, with an average spacing of ~ 4 –6 μm between the grooves is observed in the VT1-00 titanium samples after ECAP (Fig. 6a). However, typical fatigue microgrooves with a spacing of

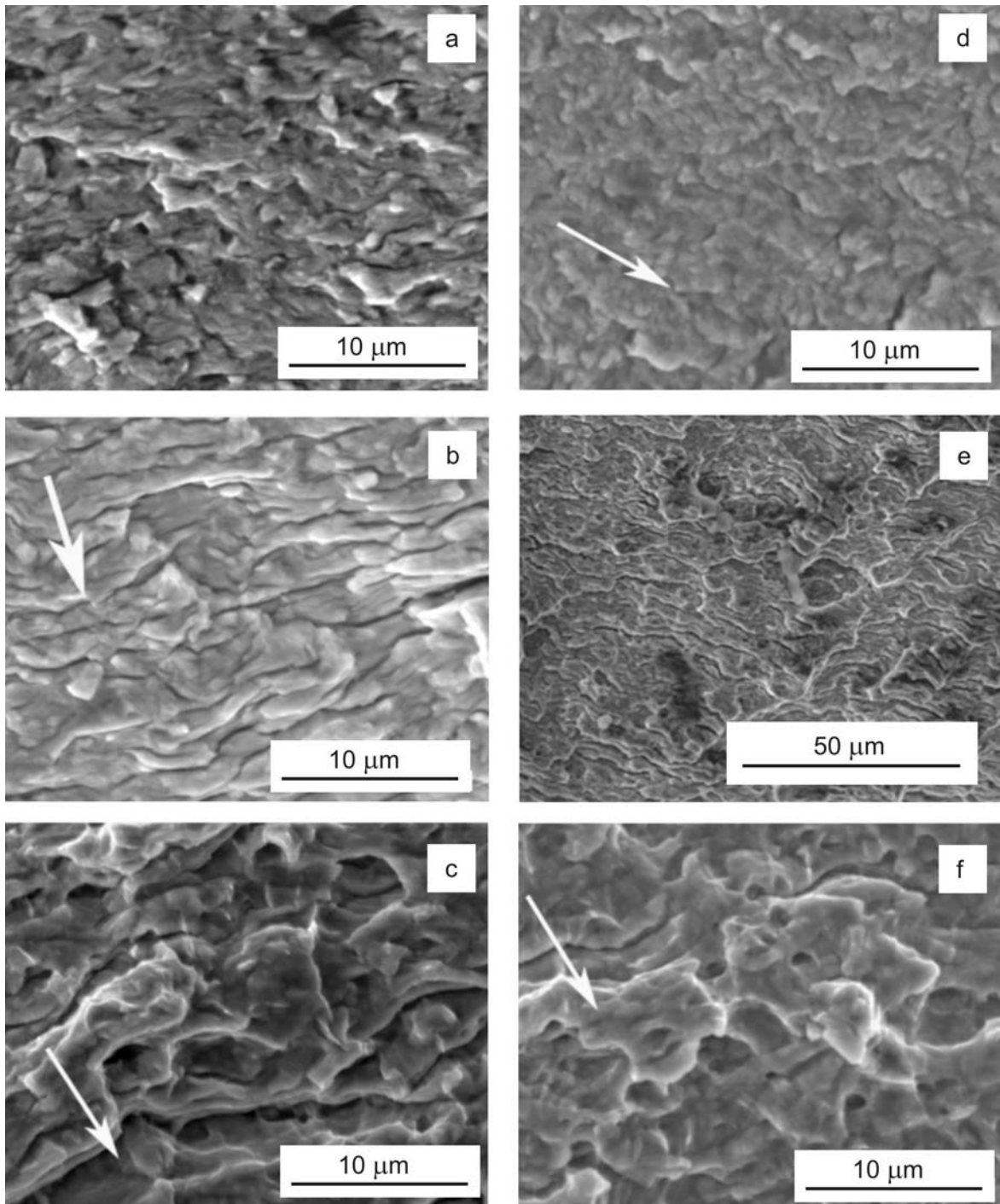


Fig. 7. Fatigue fracture surfaces of the Zr-2.5%Nb alloy samples in the initial state (a, b, c) ($\sigma_{\max} = 400$ MPa, $N = 1.1 \times 10^5$ cycles) and after ECAP (d, e, f) ($\sigma_{\max} = 420$ MPa, $N = 4.66 \times 10^6$ cycles). Arrow indicates the direction of crack propagation.

$< 1 \mu\text{m}$ between them are observed in local volumes of metal. The accelerated fatigue crack growth is connected with the transition from the lamellar relief to the ductile dimple one (Fig. 6c). The static rupture area exhibits a typical ductile dimple fracture with a dimple size of 2–5 μm , which is substantially smaller than that of the initial samples (Fig. 6d).

Figure 7 shows the failure fracture surfaces of the Zr-2.5%Nb alloy samples in the initial state and after ECAP. Just as for the commercial titanium, the macroscopic picture of the fatigue failure in both cases consists of two clear regions, i.e., the flat surface of fatigue fracture and quasi-ductile static rupture area. The regions of intergranular fracture at the boundar-

ies of blocks (granules) of $\sim 2\text{--}3\ \mu\text{m}$ in size with the traces of significant plastic deformation are observed in the initial zone of the fatigue crack propagation (Figs. 7a and 7d). At a high magnification, fatigue micro-grooves with submicron-size spacings between them are observed on the surface of the blocks.

At the stage of the stable fatigue crack propagation, quasi-ductile grooved relief with the secondary cracking at the front of the crack advance (Figs. 7b and 7e) is observed both in the initial material and in the samples subjected to ECAP; however, the relief in the ECAP samples is flatter (Fig. 7e).

A mixed fracture surface with alternating regions of quasi-ductile and ductile fracture with a dimple size of $1\text{--}3\ \mu\text{m}$ is observed in the zone of the accelerated fatigue crack growth (Figs. 7c and 7f). However, the relief is flatter in the ECAP samples. The static rupture area of the samples of both series exhibits quasi-ductile fracture (Figs. 7c and 7f).

Thus, the study of the specific features of the fatigue crack propagation mechanism in the materials under consideration showed that, in contrast to the coarse-grained metallic materials, in which the stable propagation of fatigue crack reveals the plastic grooved relief at the fracture surface, the SMC materials exhibit the mixed intergranular and ductile or quasi-ductile fracture as well as the fracture by the mechanism of the grooved relief and secondary cracking along the grooves. In this case, all microscopic elements of the fracture surface after ECAP are substantially finer.

4. Conclusions

1. The equal-channel angular pressing (ECAP) of the VT1-00 titanium and the Zr-2.5%Nb zirconium alloy substantially increases the ultimate tensile strength (by a factor of 1.6 and 1.4, respectively) and yield strength (by a factor of 2.1 and 1.6, respectively) of both materials; however, their ductility decreases more than by a factor of two.

2. The fatigue strength of both materials after ECAP reaches $\sim 400\text{--}420\ \text{MPa}$, and their σ_R/UTS ratios after ECAP are approximately similar (0.54), although, in the initial state, the static strength characteristics of the Zr-2.5%Nb alloy are higher.

3. The study of the specific features of the fatigue crack propagation mechanism in the materials under consideration showed the intergranular fracture and the fracture by the mechanism of quasi-ductile grooved relief and secondary cracking along the grooves in the SMC materials, by contrast to the coarse-grained metallic materials, in which the stable fatigue crack propagation results in the ductile grooved relief of the fracture surface.

4. In spite of significant strengthening of both ma-

terials after ECAP, they retain a sufficiently high reserve of ductility and toughness upon both static and fatigue loading.

5. As possible materials for bio-implants, both materials after ECAP do not have any advantages over each other in the level of mechanical characteristics. However, the zirconium alloy provides better biocompatibility and, therefore, along with titanium, it is a promising material for medical industry.

References

- [1] STEINEMANN, S. G.: Corrosion of Surgical Implants – In Vivo and in Vitro Tests, Evaluation of Biomaterials. New York, Wiley 1980.
- [2] FUJITA, M.: Jpn. Stomatol. Soc., 60, 1993, p. 54 (in Japanese).
- [3] ZAYMOVSKIY, A. S.—NIKULINA, A. V.—RESHETNIKOV, F. G.: Zirconium Alloys in Nuclear Industry. Moscow, Energoatomizdat 1994 (in Russian).
- [4] FADEYEV, A. YU.: Medical Equipment and Medizdeliya, 10, 2002, p. 26 (in Russian).
- [5] NIKULIN, S. A.: Zirconium Alloys for Nuclear Power Reactors. Moscow, MISiS 2007 (in Russian).
- [6] NIKULIN, S. A.—ROZHNOV, A. B.—BABUKIN, A. V.: Metallurgy and Heat Treatment of Metals, 5, 2005, p. 8 (in Russian).
- [7] PEREZ-PRADO, M. T.—GIMAZOV, A. A.—RUANO, O. A.—KASSNER, M. E.—ZHILYAEV, A. P.: Scripta Materialia, 58, 2008, p. 219.
- [8] EDALATI, K.—HORITA, Z.—YAGI, S.—MATSUBARA, E.: Mat. Sci. Eng. A, 523, 2009, p. 277. [doi:10.1016/j.msea.2009.07.029](https://doi.org/10.1016/j.msea.2009.07.029)
- [9] RYOO, H. S.—YU, H. S.—OH, K. H.—HWANG, S. K.: Material Science Forum, 408–412, 2002, p. 655. [doi: 10.4028/www.scientific.net/MSF.408-412.655](https://doi.org/10.4028/www.scientific.net/MSF.408-412.655)
- [10] PERLOVICH, Y.—ISAENKOVA, M.—FESENKO, V.—GREKHOV, M.—YU, S. H.—HWANG, S. K.—SHIN, D. H.: Materials Science Forum, 503–504, 2006, p. 859. [doi: 10.4028/www.scientific.net/MSF.503-504.859](https://doi.org/10.4028/www.scientific.net/MSF.503-504.859)
- [11] VALIYEV, R. Z.—ALEKSANDROV, I. V.: Bulk Nanostructured Metallic Materials. Moscow, IKTs AKADEMKNIGA 2007 (in Russian).
- [12] VINOGRADOV, A. YU.—HASIMOTO, S.: Metals, 2004, 1, p. 51 (in Russian).
- [13] VINOGRADOV, A.—HASHIMOTO, S.: Materials Transactions, 42, 2001, p. 74. [doi:10.2320/matertrans.42.74](https://doi.org/10.2320/matertrans.42.74)
- [14] MUGHRABI, H.: Investigations and Applications of Severe Plastic Deformation (NATO Science Series). Dordrecht – Boston – London, Kluwer Academic Publishers 2000.
- [15] HANLON, T.—TABACHNIKOVA, E. D.—SURECH, S.: International Journal of Fatigue, 27, 2005, p. 1147. [doi:10.1016/j.ijfatigue.2005.06.035](https://doi.org/10.1016/j.ijfatigue.2005.06.035)
- [16] MUGHRABI, H.—HOPPEL, H. W.: Materials Research Society Symposium Proceedings, 634, 2000, p. B2.1.1.
- [17] VINOGRADOV, A. YU.—AGNEW, S. R.: Encyclopaedia of Nanoscience and Nanotechnology. New York, Marcel Dekker 2004.

- [18] TERYENTYEV, V. F.—KOLMAKOV, A. G.—PRO-SVIRNIN, D. V.: Deformation and Fracture of Materials, 2007, 9, p. 2 (in Russian).
- [19] SEMENOVA, I. P.—YAKUSHINA, E. B.—NURGA-LEEVA, V. V.—VALIEV, R. Z.: International Journal of Materials Research, 100, 2009, p. 1691.
- [20] SEGAL, V. M.—REZNIKOV, V. I.—KOPYLOV, V. I.: Processes of Plastic Structure Formation of Metals. Minsk, Science and Technology 1994 (in Russian).
- [21] DOBATKIN, S. V.—KAPUTKINA, L. M.: Physics of Metals and Physical Metallurgy, 91, 2001, p. 79 (in Russian).
- [22] CAHN, J. W.: Acta Met., 4, 1956, p. 449.
[doi:10.1016/0001-6160\(56\)90041-4](https://doi.org/10.1016/0001-6160(56)90041-4)
- [23] GORELIK, S. S.—DOBATKIN, S. V.—KAPUTKI-NA, L. M.: Recrystallization of Metals and Alloys. Moscow, MISIS 2005 (in Russian).
- [24] FARBER, V. M.: Physical Metallurgy and Heat Treatment of Metals, 2002, 8, p. 3 (in Russian).
- [25] DOHERTY, R. D.—SZPUNAR, J. A.: Acta Met., 32, 1984, p. 1789. [doi:10.1016/0001-6160\(84\)90235-9](https://doi.org/10.1016/0001-6160(84)90235-9)
- [26] ROSSARD, C.—LE BON, A.—THIVELLIER, D.—MANENC, J.: Met. Sci. Rev. Met., 66, 1969, p. 263.
- [27] BERNSHTEIN, M. L.—DOBATKIN, S. V.—KA-PUTKINA, L. M.—PROKOSHKIN, S. D.: Diagrams of Hot Deformation, the Structure and Properties of Steels. Moscow, Metallurgiya Publ. 1989 (in Russian).
- [28] ZHERNAKOV, V. S.—LATYSH, V. V.—STOLYA-ROV, V. V.—ZHARIKOV, A. I.: In: Proc. of the Fourth Conference on Nanostructured Materials (NANO-98). Stockholm, Royal Inst. Technol. 1998, p. 609.
- [29] KIM, W.-J.—HYUN, C. Y.—KIM, H. K.: Scr. Mater., 54, 2006, p. 1745.
[doi:10.1016/j.scriptamat.2006.01.042](https://doi.org/10.1016/j.scriptamat.2006.01.042)
- [30] VINOGRADOV, A.—STOLYAROV, V. V.—HASHI-MOTO, S.—VALIEV, R. Z.: Materials Science and Engineering A, 318, 2001, p. 163.
[doi:10.1016/S0921-5093\(01\)01262-X](https://doi.org/10.1016/S0921-5093(01)01262-X)
- [31] VALIEV, R. Z.—SEMENOVA, I. P.—JAKUSHINA, E.: Nanomaterials by Severe Plastic Deformation IV. Part 1. Eds.: Estrin, Y., Maier, H. J. Uetikon-Zurich, Trans Tech Publications Ltd 2008.
- [32] SEMENOVA, I. P.—SALIMGAREYEVA, G. KH.—LATYSH, V. V.—KUNAVIN, S. A.—VALIEV, R. Z.: Physical Metallurgy and Heat Treatment of Metals, 644, 2009, p. 34.